Chapter 2

Results and Discussion

A comparative study of ball-milled FM powders (Co or $SmCo_5$) alone and together with AFM (NiO) powders, in different weight ratios, is presented. Some reviews on materials processing by means of mechanical milling can be found elsewhere [57]. The different structural and magnetic behaviors of Co and $SmCo_5$ when subjected to ball milling or heat treatments makes it necessary to adapt in each case the processing route to optimize the effects of the coupling. In the case of ball milled Co + AFM (NiO or FeS) a heat treatment process (annealing + field cooling to room temperature) of the as-milled powders is needed in order to induce FM-AFM exchange interactions which result in an improvement of the magnetic properties. However, in the case of ball milled $SmCo_5$ + AFM powders, heating results in a rapid deterioration of the hard ferromagnetic properties, mainly due to the formation, at intermediate temperatures, of non-magnetic or softer phases (Sm_2Co_7 or Sm_2Co_{17}), which cause a loss of the magnetic anisotropy. Moreover, annealing of $SmCo_5$ + NiO can also result in the oxidation of Sm, since Sm is more reactive with oxygen than Ni or Co. However, the local heating during the milling, due to the impacts between powders and balls, together with the microscopic fields originating from the hard FM $SmCo_5$ particles, makes it possible to observe some effects from FM-AFM coupling in the as-milled state, without need of any posterior heat treatment process.

The magnetic results have been correlated with the microstructure developed in each case during the milling process. The morphology of the particles has been characterized by means of scanning electron microscopy (SEM) and energy dispersive x-ray (EDX) analyses [58]. Structural characterization has been performed using x-ray diffraction (XRD) [59]. From the patterns, which have been fitted using a full-pattern fitting procedure (Rietveld method), the crystallite sizes and microstrains have been determined at the different stages of milling [60,61]. Magnetic hysteresis loops have been carried out using a vibrating sample magnetometer (VSM) [62], up to 1.1 T, and an extraction magnetometer [63], up to 20 T, for Co-NiO and $SmCo_5$-NiO, respectively. In the latter case, the large magnetic anisotropy of $SmCo_5$ makes it necessary to use a high field magnetometer in order to ensure complete saturation of the powders and hence have reliable values of coercivity.

1.- Morphological Characterization

SEM observations reveal that the starting Co and $SmCo_5$ particles are irregular-shaped and have sizes of up to 40 and 500 μm, respectively. When they are ball milled alone, they are progressively reduced in size and tend to become elongated, due to their ductile character, turning into small platelet-shaped particles of a few μm in size. For example, shown in figure 2.1 are the SEM images (obtained from secondary electrons) of Co particles, before milling (a) and after milling for 20h (b).

(a)

(b)

Figure 2.1: SEM images (secondary electrons) of Co particles before milling and after milling for 20 h.

However, when the FM particles are ball milled with NiO a different microstructure is found. In this case, in order to observe the FM-AFM interfaces, the as-milled powders have been embedded in epoxy resin and subsequently polished with diamond paste. For a detailed description of the microstructure developed by ball milling, either in Co or $SmCo_5$ alone or with the AFM, the reader is referred for example to papers III, IV, V, VII and VIII in chapter

3. The SEM images (backscattered electrons) of Co-NiO ball milled in the 1:1 weight ratio for 0.1, 1 and 20 h are shown in figure 2.2.

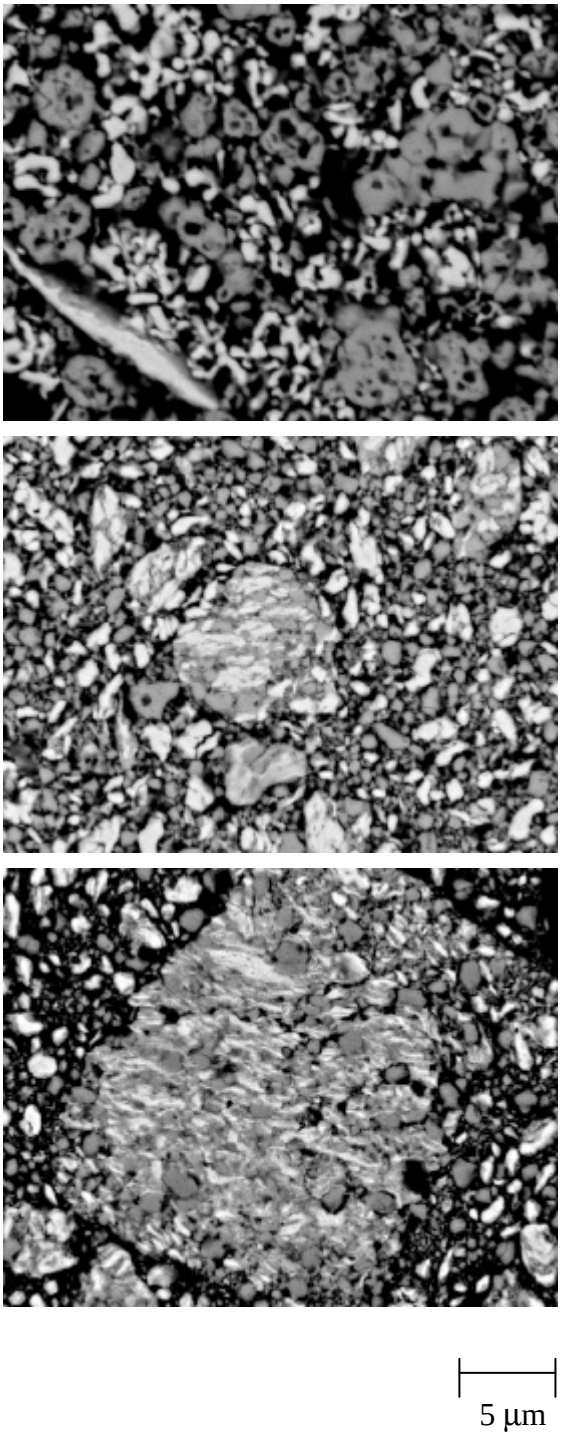

Figure 2.2: SEM images (backscattered electrons) of Co + NiO powders milled for 0.1, 1 and 20 h, in the weight ratio 1:1.

It can be seen that after milling for 0.1 h, the Co and NiO powders are well-mixed but still remain independent, i.e. not soldered together. Therefore the amount of interfaces between Co and NiO for short milling times is small. As the milling time increases, due to their ductile character, Co particles start to deform and lamellar shapes are developed, while NiO particles are progressively fractured and reduced in size. At the same time, Co and NiO grains tend to solder together and, after milling for 1 h, one obtains FM-AFM aggregates of sizes between 1 and 5 μm. After milling for 20 h a large number of agglomerates consisting of Co lamellae embedded in a NiO matrix are formed and the sizes of some of them reach 30 μm. This microstructure, typical of ball milled metal-ceramics, allows a large number of FM-AFM interfaces to be developed, at which the coupling will be induced. A similar microstructure (i.e. FM grains embedded in an AFM matrix) is also observed in $SmCo_5$ + NiO after intermediate milling times (e.g. after a few hours milling). The size of the agglomerates is found to increase with milling time. EDX mappings, like the ones shown in figure 2.3 (b,c,d), reveal that the bright particles in figure 2.2 effectively correspond to the metallic FM (Co or $SmCo_5$), while the gray ones to NiO (the black zones are mainly epoxy resin).

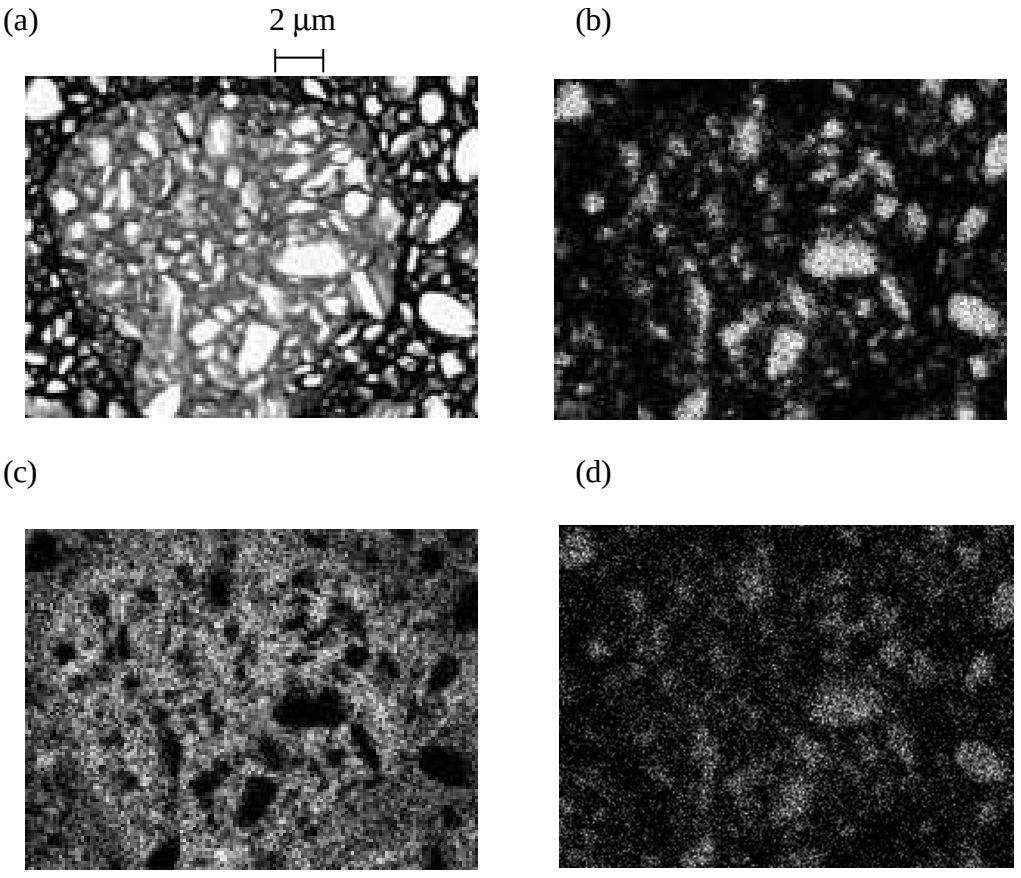

Figure 2.3: (a) SEM image (backscattered electrons) with the corresponding Co (b), Ni (c) and Sm (d) EDX mappings for $SmCo_5$ ball milled with NiO for 32 h, in the weight ratio 1:1.

It is also noteworthy that the sharp contrast obtained in the EDX analyses indicates that the amount of atomic interdiffusion between the FM and AFM components is small.

2.- Structural Characterization:

2.1.- The case of Co-NiO

Cobalt is found to undergo structural changes and phase transitions during ball milling [64,65]. XRD patterns of pure Co reveal that the starting powders are a mixture of hcp and fcc phases. As the milling time increases the amount of fcc-Co is found to drastically decrease, vanishing almost completely after 1 h of milling. For longer milling times, the percentage of fcc-Co (which is usually only stable above 700 K) increases again, basically due to the formation of large amounts of stacking faults in the hcp structure.

Shown in figure 2.4 are the XRD patterns of unmilled NiO (a), unmilled Co (b) and 1 h ball milled Co (c) and 20 h ball milled Co + NiO (d). The XRD pattern of NiO is the typical of a fcc structure. However, for Co a mixture of two phases, hcp+fcc, is observed. The subindexes H and C denote hpc and fcc Co, respectively. The Miller indexes (*h*,*k*,*l*), for both Co and NiO, are also indicated in the figure. It can be observed that Co peaks in the original powder (curve (b)) are relatively wide, probably due to the large amounts of defects introduced in its structure during the gas atomization process. Furthermore, it is found that, even in the unmilled Co powder, the hcp peaks satisfying the condition $h - k = 3n \pm 1$ (being n an integer) are extra-broadened. This is due to the existence of stacking faults in the hcp-Co structure [66]. After milling Co for 1 h, the peak $(200)_{Co,C}$ disappears, indicating the existence of an allotropic phase transformation from fcc to hcp-Co during the first stages of milling. For longer milling times, a large amount of defects, specially stacking faults, are introduced in hcp-Co. Therefore, the hcp stacking sequence …ABABABABAB… changes into a disordered …ABAB**ABCA**BABAB…, where the bold letters indicate the formation of a local fcc stacking sequence. This shows that, due to the milling, some small crystallites with fcc structure are created in the hcp phase. As a result, a wide hump is observed for long milling times at the position corresponding to the $(200)_{Co,C}$ peak (see curve (d) in figure 2.4).

When Co is milled together with NiO the intensity of fcc-Co diffraction peaks also decreases rapidly with milling time, indicating that the transformation from fcc to hcp-Co also takes place when Co and NiO are milled together. For further description of the milling-induced allotropic transformation of Co, either when milled alone or with NiO, see papers I-V in chapter 3.

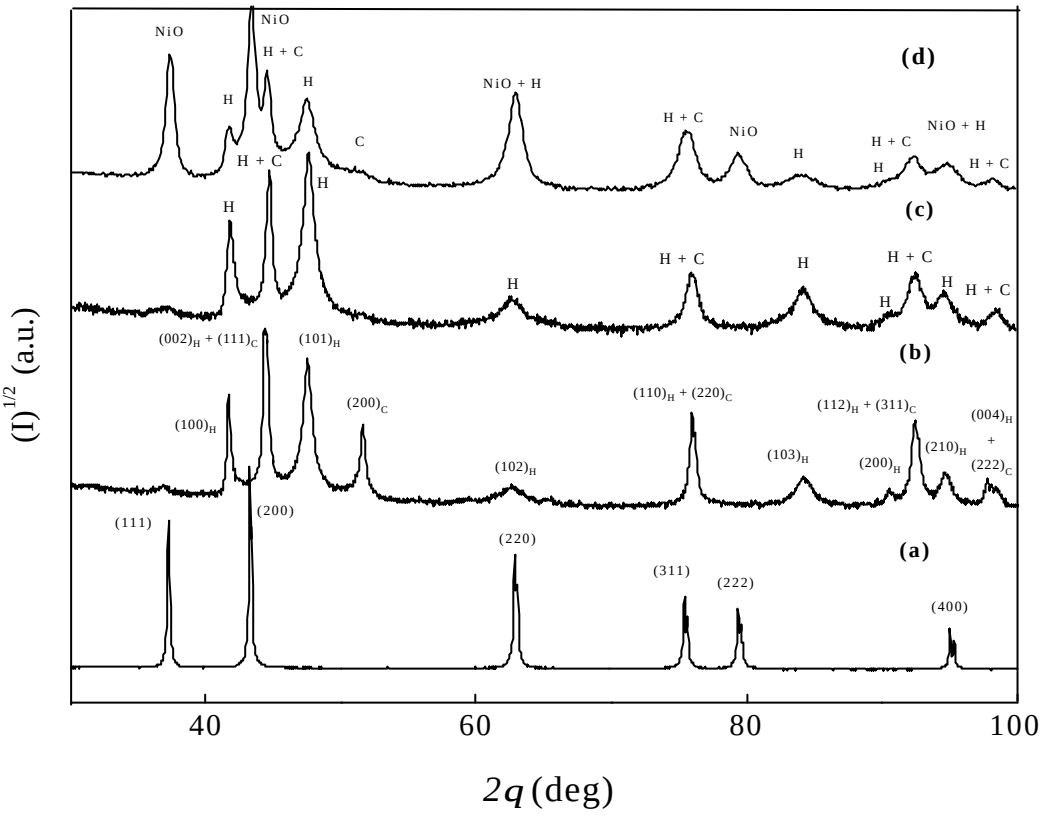

Figure 2.4: XRD patterns of (a) unmilled NiO, (b) unmilled Co, (c) 1 h ball milled Co and (d) 20 h ball milled Co + NiO in the weight ratio 1:1.

It is also remarkable that during ball milling the position of the XRD peaks, for both Co and NiO remain essentially unchanged, indicating that the cell parameters do not change substantially. Therefore, the amount of atomic interdiffusion between both components is small. However, the XRD peaks are found to be progressively broadened as the milling time is increased. This is due to the decrease of crystallite size and the increase of microstrains. Moreover, the crystallite size reduction associated with the milling process is steeper when Co is milled alone and it becomes less abrupt as the NiO content is increased, indicating that milling with NiO slows down Co structural changes.

Shown in figure 2.5 are the XRD patterns of 20 h ball milled Co, before annealing (a) and after annealing for 0.5 h and field cooling to room temperature (H = 5 kOe) from two different temperatures, i.e. 600 K (curve (b)) and 740 K (curve (c)). In curve (b) it can be observed that after annealing at T = 600 K, NiO and Co peaks are not shifted in angle. However, there is a decrease of the peak width, due to a slight increase of the crystallite size. Moreover, after annealing at T = 600 K Co powders are still basically in the hcp form. On the contrary, annealing at 740 K causes a certain amount of hcp-Co to allotropically transform

into fcc. Moreover, annealing at higher temperatures, apart from inducing the hcp to fcc transformation, it also brings about a drastic increase of the crystallite size in the hcp phase, from approximately 10 nm in the as-milled state to 18 nm after annealing at 740 K. It is also worth mentioning that annealing at T = 600 K or 740 K does not result in formation of Co oxides, such as CoO or Co_3O_4.

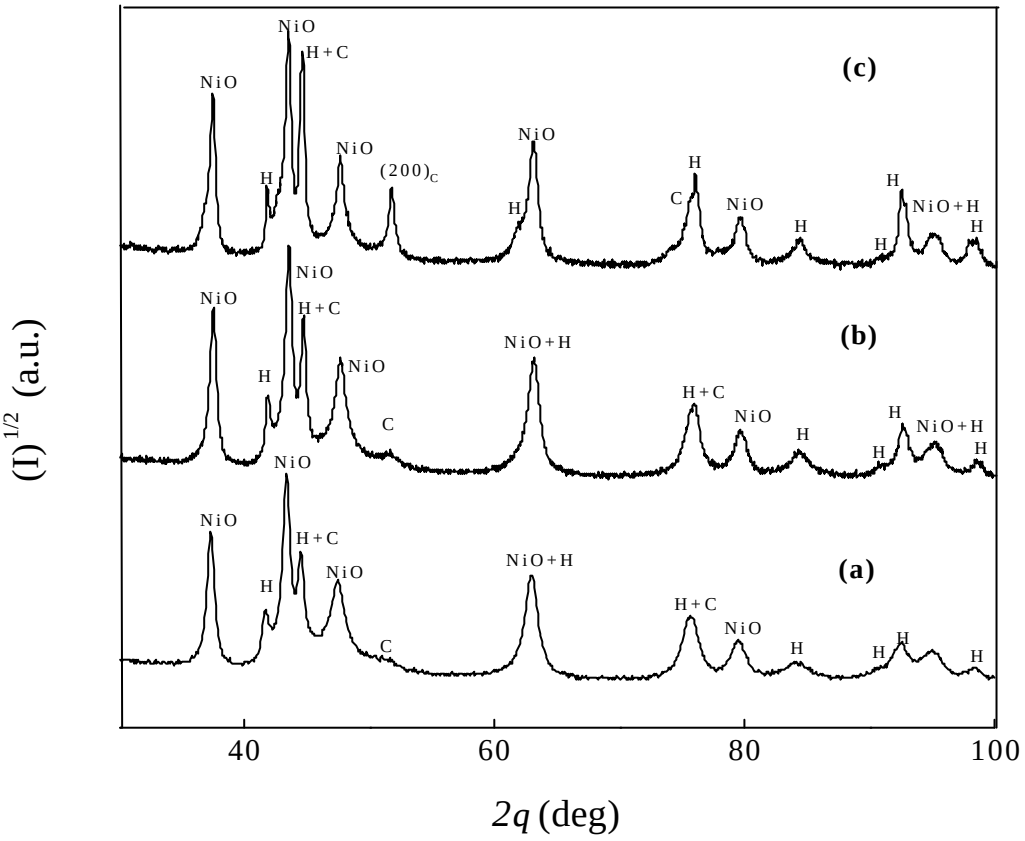

Figure 2.5: XRD patterns of 20 h ball milled Co + NiO, in a weight ratio of 1:1, before annealing (a) and after annealing and field cooling (H = 5 kOe) from T = 600 K (b) and T = 740 K (c).

2.2.- The case of $SmCo_5$-NiO

Shown in figure 2.6 are the XRD patterns of $SmCo_5$ milled with NiO for 0.25, 4 and 32 h. As for Co-NiO it can be observed that, as the milling time increases, the XRD peaks of both $SmCo_5$ and NiO progressively broaden, indicating a reduction of the crystallite size and an increase of microstrains (see figure 2.6). In fact, as shown in figure 2.7, the reduction of crystallite size is rather steep for short milling times, although it tends to level off for longer

milling times. Also from figure 2.7 it can be seen that, as the NiO content increases, the crystallite size reduction during the milling becomes smoother. For example, it is noteworthy that the crystallite size for $SmCo_5$ milled alone, after long-term milling (e.g. 32 h), is much smaller when milled alone ($<D>$ = 2.5 nm) than when milled with NiO, i.e. $<D>$ = 9 nm for $SmCo_5$(1):(1)NiO.

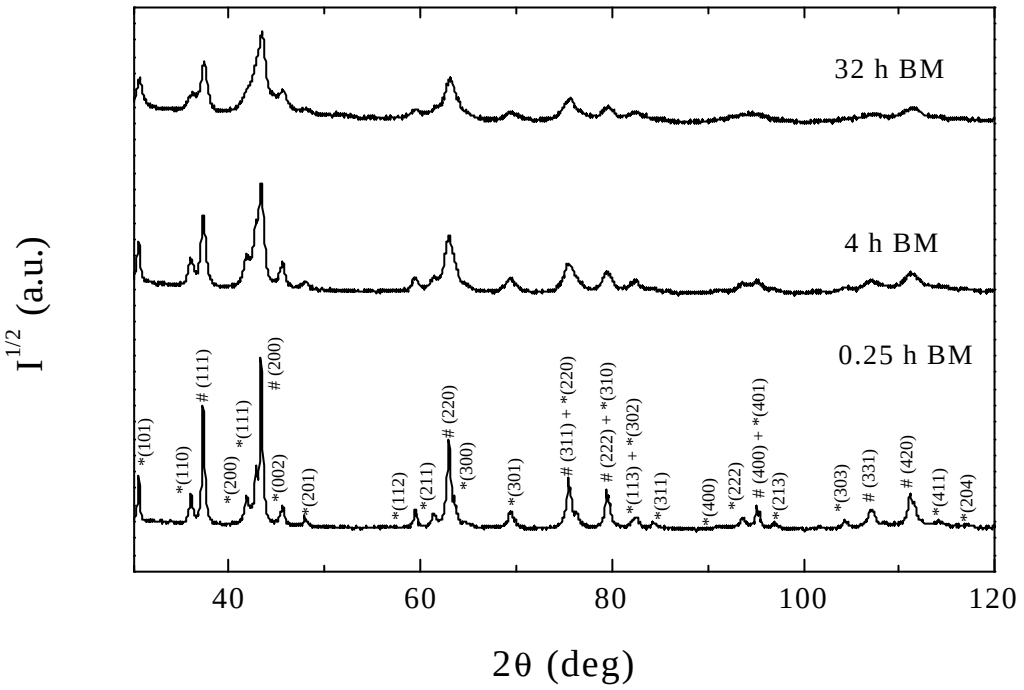

Fig. 2.6: X-ray diffraction patterns of $SmCo_5$ + NiO ball milled during 0.25, 4 and 32 h, in the weight ratio 1:1. The symbols ∗ and # denote $SmCo_5$ and NiO peaks, respectively. Their Miller indexes are also indicated.

In addition, the microstrains, $<e^2>^{1/2}$, also increase with milling time and, after prolonged milling, $<e^2>^{1/2}$ is found to be slightly larger in $SmCo_5$ than for $SmCo_5$ + NiO. This is an indication that large amounts of structural defects, such as dislocations or vacancies, are introduced in the material during the milling. The small crystallite size and the large microstrain for $SmCo_5$ milled alone indicate that after 32 h $SmCo_5$ is close to amorphization, as already reported by other groups. Nevertheless, as in the case of Co + NiO, the milling appears to be less aggressive when $SmCo_5$ is milled with NiO. For further description of the structural evolution of $SmCo_5$ + NiO during the milling, the reader is referred to papers VI-IX in chapter 3.

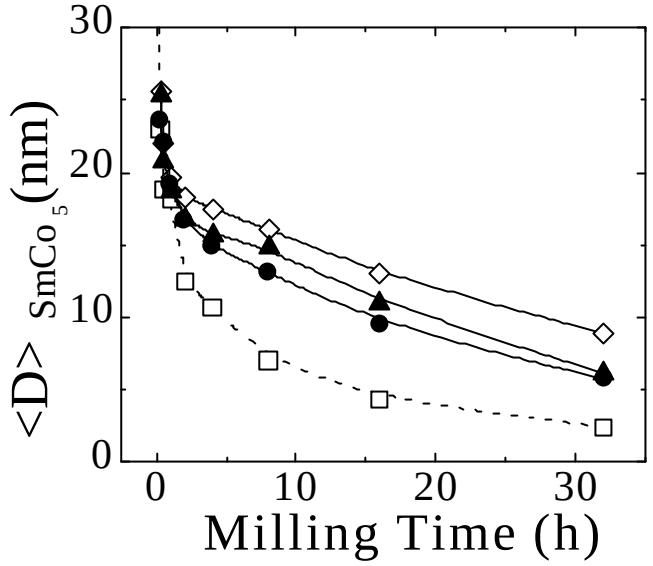

Figure 2.7: Milling time dependence of the $SmCo_5$ crystallite size, $<D>_{SmCo5}$ for the $SmCo_5$:NiO weight ratios 1:0 (-- □ --), 3:1 (— ● —), 3:2 (— ▲ —) and 1:1 (— ◇ —). Note that, for clarity, the crystallite size of the starting $SmCo_5$ powders ($<D>_{SmCo5,\ initial}$ = 43.4 nm) has not been plotted.

3.- Magnetic Characterization:

3.1.- The case of Co-NiO

To demonstrate the existence of FM-AFM exchange interactions in ball milled Co-NiO we have compared the magnetic behaviours of Co milled alone and with NiO. This is presented in papers I-V of chapter 3. Shown in figure 2.8 is the magnetic dependence of coercivity of as-milled Co powders, before annealing and after annealing at 600 K for 0.5 h and field cooling (H = 5 kOe) to room temperature. It can be seen that H_C first increases with milling time, reaching a maximum after 1 h of milling and then it starts to decrease for longer milling times. The increase of H_C for short milling times is mainly attributed to the transformation of the starting mixture of hcp+fcc Co to an almost pure hcp phase, since hcp-Co has higher magnetic anisotropy.

The decrease of H_C for longer milling times is probably linked with the formation of a large amount of defects (basically stacking faults) in the hcp structure and the subsequent

appearance of fcc crystallites, which is known to decrease the magnetocrystalline anisotropy of Co [2-5].

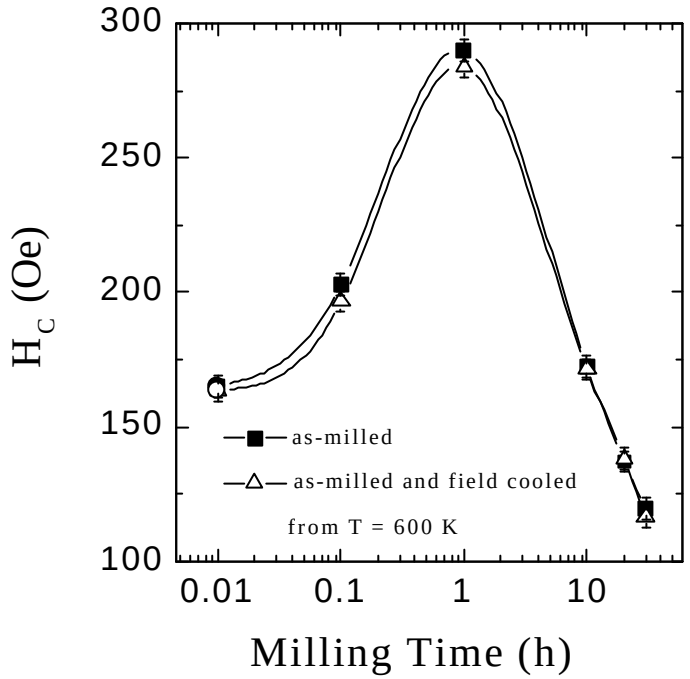

Figure 2.8: Milling time dependence of H_C (measured at room temperature) for Co powders, before annealing (-■-) and after annealing for 0.5 h at T = 600 K and field cooling to room temperature (H = 5 kOe) (-△-).

The most remarkable aspect of figure 2.8 is that, after annealing and field cooling from T = 600 K, H_C is virtually unchanged with respect to that of the as-milled powders. Only a slight decrease of H_C is observed, which can be understood in terms of crystallite size increase or a small transformation of hcp to fcc Co.

Nevertheless, the magnetic behaviour of Co milled with NiO is completely different. Shown in figure 2.9 is the milling time dependence of H_C for ball milled Co + NiO in a weight ratio of 1:1. As in the case of ball milled Co alone, a maximum is observed when plotting H_C as a function of milling time. But, in this case, the maximum appears after a longer milling time, i.e. 20 h, confirming that NiO slows down Co structural changes during the milling.

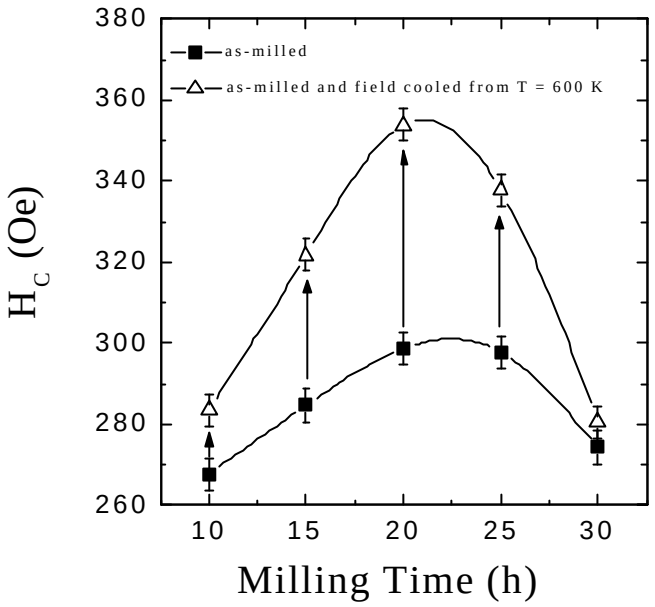

Figure 2.9: Milling time dependence of H_C (measured at room temperature) for ball milled Co + NiO powders (1:1 weight ratio), before annealing (-■-) and after annealing for 0.5 h at T = 600 K and field cooling to room temperature (H = 5 kOe) (-△-).

Moreover, contrary to ball milled Co alone, annealing for 0.5 h at T = 600 K and field cooling to room temperature (H = 5 kOe), results in a significant enhancement of H_C, for milling times longer than 10 h. Therefore it is clear that NiO plays an important role in enhancing H_C of ball milled Co, since it has been demonstrated by XRD that annealing at T = 600 K does not bring about significant structural changes in Co. Thus, the H_C enhancement is mainly a magnetic and not a structural effect.

To better understand the role of NiO in enhancing H_C, the 20 h ball milled Co + NiO powders have been annealed and field cooled from different temperatures, 300 K < T_{ANN} < 750 K. The dependence of H_C on T_{ANN} is shown in figure 2.10. It can be seen that H_C reaches a maximum value for T_{ANN} ~ 600 K, just above NiO Néel temperature (T_N = 590 K). This is in agreement with the intuitive picture of FM-AFM coupling that has been reported in chapter 1 and with many experimental results obtained in fine particles (at temperatures below room temperature) or in thin films (at room temperature or below) [22]. The fact that H_C is only enhanced for $T_{ANN} > T_N$ is the first experimental evidence that FM-AFM exchange interactions can be induced between Co and NiO by means of ball milling and subsequent heat treatments. It is noteworthy that annealing and field cooling ball milled Co powders (without the presence of AFM NiO) only results in a progressive decrease of H_C as T_{ANN} is increased.

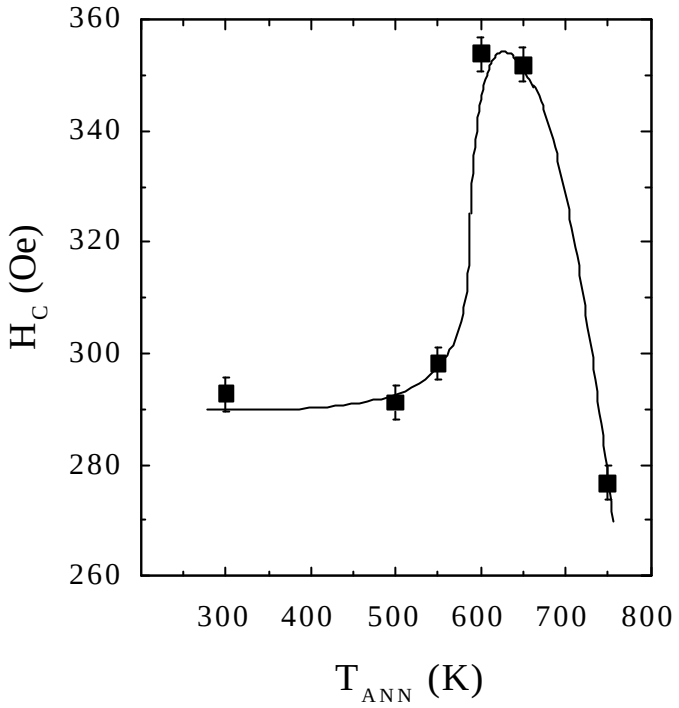

Figure 2.10: Dependence of H_C on the annealing temperature, T_{ANN}, for 20 h ball milled Co + NiO (in a weight ratio of 1:1). The as-milled powders were annealed for 0.5 h at T_{ANN} and subsequently field cooled (H = 5 kOe) to room temperature.

In figure 2.10 it can also be seen that if T_{ANN} is too high (above 650 K) H_C is significantly reduced. This can be understood as a consequence of the allotropic phase transformation that occurs in Co (from hcp to fcc phase) when heated to above the transition temperature, T_t, which is usually around 700 K [68]. However, this temperature can be considerably lowered as the particle size is reduced [69].

Similar dependences of H_C on T_{ANN} have also been found in Co + NiO for other milling times, as far as they are longer than 10 h. This means that FM-AFM coupling is induced, to a certain extent, after milling for 10 h (and posterior field cooling) [70].

Further evidence for FM-AFM exchange interactions comes from the observation of shifted hysteresis loops (along the field axis), after field cooling from above T_N (NiO). The dependence of the loop shift, H_E, on T_{ANN} for 20 h ball milled Co + NiO is shown in figure 2.11.

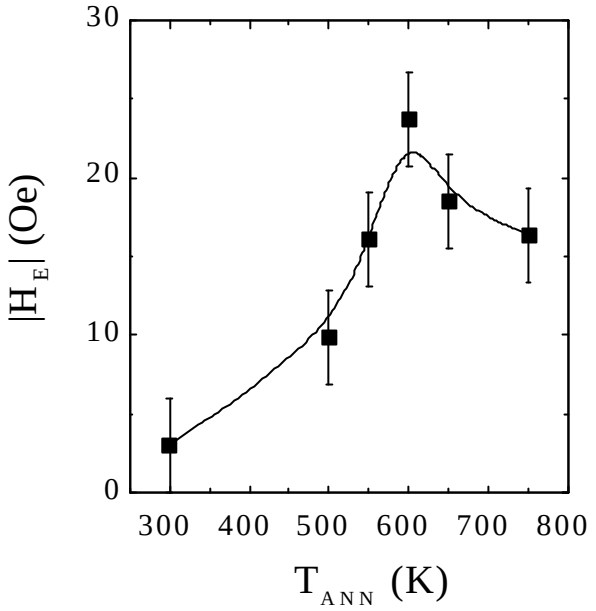

Figure 2.11: Dependence of H_E on the annealing temperature, T_{ANN}, for 20 h ball milled Co + NiO (in a weight ratio of 1:1). The as-milled powders were annealed for 0.5 h at T_{ANN} and subsequently field cooled (H = 5 kOe) to room temperature.

The dependence of H_E on T_{ANN} is similar to that of H_C, i.e. a maximum is observed for T_{ANN} T_N. Also noticeable is that for $T_{ANN} < T_N$ small loop shifts are observed. In fact, due to thermal fluctuations, the AFM tends to magnetically disorder as temperature increases. Actually, the temperature at which FM-AFM exchange interactions effects disappear is sometimes lowered with respect to T_N, especially for very small AFM particles [22]. Moreover, in our case H_E is found to be relatively small, compared to H_C. A similar result has been obtained in Ni-NiO fine powders [46] and Co-NiO thin films [71]. This is typical for systems in which the AFM anisotropy is relatively low (e.g. $K_{NiO} < 5 \times 10^4$ erg/cm^3).

Besides the H_C enhancement, it has been observed that the squareness ratio, M_R/M_S, also increases in ball milled Co-NiO, compared to ball milled Co, after field cooling from $T > T_N$. Moreover, the dependence of M_R/M_S on T_{ANN} has been found to be similar to that of H_C or H_E, suggesting that, although the origin of the M_R/M_S enhancement still remains somewhat unclear, it can be related, at least in part, to the existence of FM-AFM interactions. For example, it could be argued that, during the hysteresis loop, due to the FM-AFM exchange interactions, when the magnetic field is removed, the spins in the FM located at the interfaces with the AFM could, to some extent, remain aligned in the direction of the previous magnetizing field, thus increasing M_R/M_S. It is noteworthy that M_R/M_S enhancements have been also occasionally observed in other FM-AFM systems [72].

The FM:AFM weight ratio has also been varied in order to try to further increase H_C. For all compositions studied (FM:AFM ratios of 1:0, 7:3, 3:2, 1:1 and 2:3), H_C is found to first increase with the milling time and then progressively decrease, due to the structural changes occurring in Co when subjected to ball milling. However, the milling time corresponding to maximum H_C in each case, t_{Max}, is found to shift towards higher values as the NiO content increases. This is mainly due to the role of NiO in slowing down Co structural changes during the milling. A summary of the magnetic properties of ball milled Co + NiO, for different compositions, before and after field cooling (F.C.), is shown in table 2.1. Apart from t_{Max}, H_C (before and after F.C. from T_{ANN} = 600 K) and H_E (after F.C.), also the values of coercivity enhancement, ΔH_C = H_C (after F.C.) – H_C (before F.C.) and the energy product, $(BH)_{Max}$ (after F.C.), corresponding to t_{Max}, are shown in table 2.1 as a function of the FM:AFM percentages.

% (weight) Co	t_{Max} (h)	H_C (t_{Max}) (± 10 Oe) [before F.C.]	H_C (t_{Max}) (± 10 Oe) [after F.C.]	ΔH_C (t_{Max}) (± 7 Oe)	H_E (t_{Max}) (± 7 Oe) [after F.C.]	$(BH)_{Max}$ (t_{Max}) (G.Oe · 10^4) [after F.C.]
100 (1:0)	1	288	284	-4	2	7.1 ± 0.7
70 (7:3)	12.5	280	309	29	8	7.6 ± 0.7
60 (3:2)	17.5	302	330	28	10	8.3 ± 0.7
50 (1:1)	22.5	297	344	47	22	6.2 ± 0.6
40 (2:3)	25	264	280	16	8	2.9 ± 0.5

Table 2.1: Summary of the magnetic properties of ball milled Co + NiO, measured at room temperature, for different FM:AFM weight ratios, where t_{Max} is the milling time corresponding to the maximum ΔH_C in each composition. All values of H_C, H_E and $(BH)_{Max}$ are given for t_{Max}.

From the table it is clear that, for all compositions, except for pure Co, an enhancement of H_C and a loop shift is observed after annealing and field cooling from T_{ANN} = 600 K. The maximum ΔH_C and H_E are obtained for the FM:AFM ratio of 1:1.

As mentioned in chapter 1, the magnitude that determines the quality of a permanent magnet is the energy product, $(BH)_{Max}$. The role of NiO in enhancing $(BH)_{Max}$ is discussed in papers II and V of chapter 3. Shown in figure 2.12 is the dependence of $(BH)_{Max}$ on the NiO content, after milling during t_{Max}, before and after annealing for 0.5 h at T_{ANN} = 600 K and field cooling to room temperature (H = 5 kOe). In as-milled powders, $(BH)_{Max}$ tends to decrease as the NiO content increases, essentially because of the decrease of the overall M_S, due to the zero net magnetization of the AFM. Nevertheless, after

field cooling the powders, one observes for all compositions (except for pure Co) an enhancement of $(BH)_{Max}$, mainly due to the enhancements of H_C and M_R/M_S resulting from the FM-AFM exchange interactions. It is noteworthy that, although the maximum H_C enhancement is obtained for the weight ratio 1:1, $(BH)_{Max}$ is further enhanced for the FM(3):(2)AFM ratio. This is because of the two-fold role of the AFM. On the one hand, higher NiO contents bring about a higher $(BH)_{Max}$ because of the increase of FM-AFM interactions. On the other hand, if the AFM content is too high, the effects of the coupling are not enough to overcome the reduction of M_S and, thus, $(BH)_{Max}$ is not enhanced.

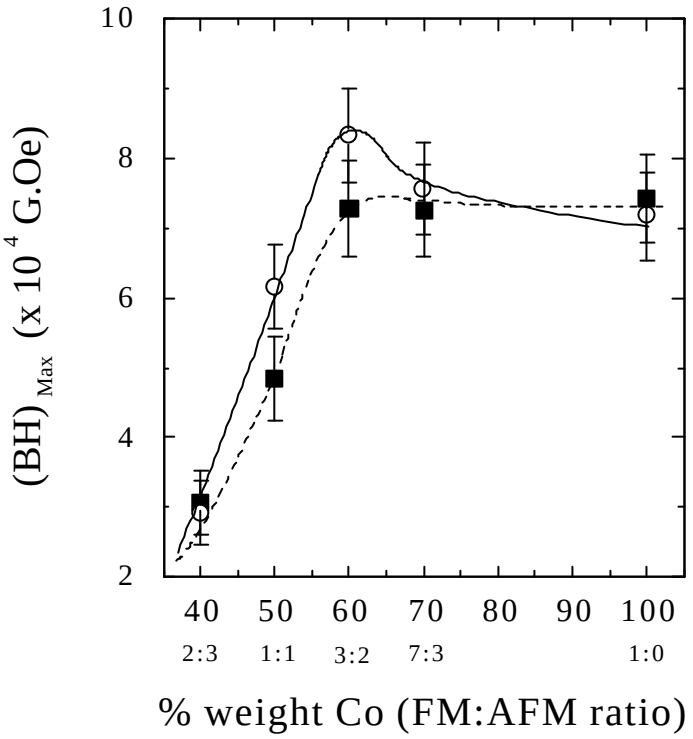

Figure 2.12: Dependence of the energy product, $(BH)_{Max}$ (measured at room temperature), on the NiO content, before (-■-) and after (-○-) annealing for 0.5 h at T_{ANN} = 600 K and field cooling (H = 5 kOe) to room temperature.

The thermal dependences of loop shift and coercivity enhancement have also been studied in papers II, IV and V of chapter 3. Since the coupling depends on the spin configurations at the interfaces between the FM and AFM components, it is reasonable to assume that thermal energy will have an influence on the coupling between them, i.e. the effects of coupling will tend to decrease as temperature is increased, because of the loss of magnetic order in the FM and AFM materials. To analyze the effect of temperature, hysteresis

loops of the 20 h ball milled Co + NiO powders (weight ratio 1:1) have been measured at different temperatures (T > 300 K) before and after annealing at T_{ANN} = 600 K and field cooling to room temperature (H = 5 kOe). Shown in figure 2.13 are the thermal dependences of ΔH_C, H_E and $\Delta(BH)_{Max}$, where $\Delta(BH)_{Max}$ is defined as $(BH)_{Max}$ (after annealing) – $(BH)_{Max}$ (before annealing).

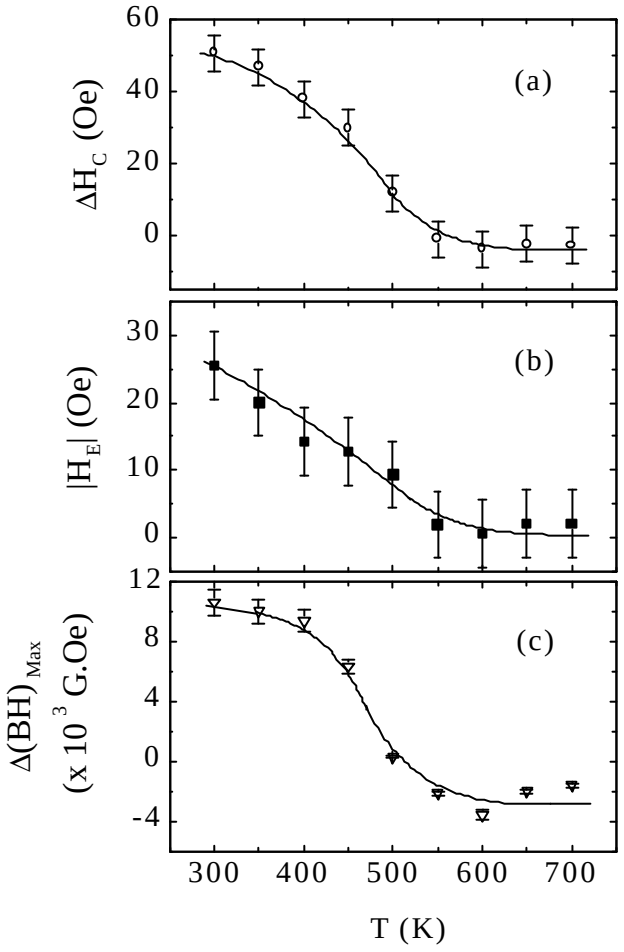

Figure 2.13: Thermal dependences of (a) coercivity enhancement, ΔH_C, (b) loop shift, H_E, and (c) enhancement of the energy product, $\Delta(BH)_{Max}$, of Co ball milled with NiO for 20 h, in the weight ratio of 1:1, measured all of them at the temperature T. Note that ΔH_C and $\Delta(BH)_{Max}$ have been obtained by taking the difference of H_C and $(BH)_{Max}$, between after and before annealing for 0.5 h at T_{ANN} = 600 K and field cooling to room temperature (H = 5 kOe).

It can be seen from figure 2.13 that the three quantities (ΔH_C, H_E and $\Delta(BH)_{Max}$) progressively reduce as temperature is increased, vanishing almost completely for $T \geq 600$ K. This is typical of FM-AFM exchange coupled systems: the coupling decreases with

temperature because of the loss of magnetic order in the AFM and the decrease of AFM magnetocrystalline anisotropy.

Finally, it is interesting to mention that same processing route than in Co + NiO has also been applied to Co+FeS and some evidences of FM-AFM exchange interactions induced by ball milling (such as the presence of loop shifts or coercivity enhancements) have also been observed (see paper I in chapter 3). For example, from the curve H_C vs. T_{ANN} (for 10 h ball milled Co+FeS in a weight ratio of 1:1), a maximum in H_C has also been observed at T_{ANN} = 650 K. The fact that the maximum appears at T_{ANN} = 650 K (and not at T_{ANN} = 600 K, like in Co-NiO) is attributed to the difference in Néel temperatures between NiO and FeS, i.e. T_N (NiO) = 590 K, while T_N (FeS) = 613 K. Therefore, H_C is only enhanced after field cooling from above T_N (FeS), as expected from FM-AFM exchange coupling.

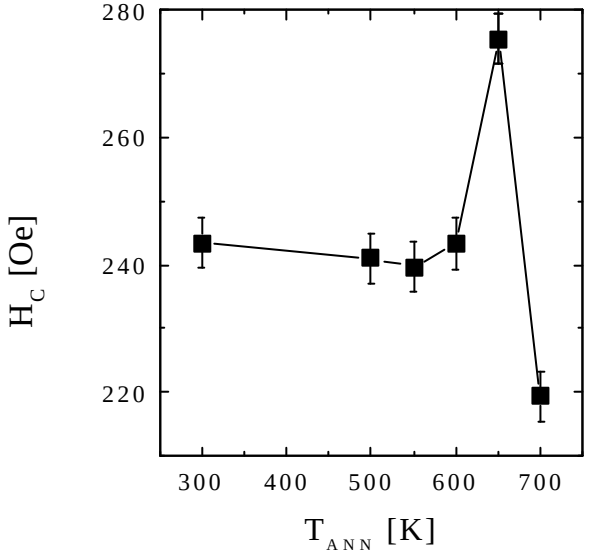

Figure 2.14: Dependence of H_C, measured at room temperature, on the annealing temperature, T_{ANN}, for Co+FeS milled for 10 h in the weight ratio of 1:1. The as-milled powders were annealed for 0.1 h at T_{ANN} and subsequently field cooled to room temperature (H = 5 kOe), previously to the magnetic measurements.

3.2.- The case of $SmCo_5$ + NiO:

When $SmCo_5$ + NiO is subject to heat treatments at temperatures above the T_N (NiO) to induce FM-AFM coupling, it results in a substantial decrease of H_C, M_S and consequently of $(BH)_{Max}$. This effect has a structural origin, rather than a magnetic one. Although this effect has not been examined in detail in the present work, several authors have reported that, when

$SmCo_5$ is heated to intermediate temperatures, there is a progressive loss of its magnetocrystalline anisotropy, mainly due to the segregation of softer phases or even non-magnetic phases, such as Sm_2Co_{17} or Sm_2Co_7 [67]. In addition, we have observed that, in annealed $SmCo_5$ + NiO powders, even when heat treatments are performed under high vacuum conditions (10^{-5} mbar), Sm is always partially oxidized, probably due to reaction with oxygen from NiO.

Nevertheless, both H_C and M_R/M_S, are found to considerably enhance in *as-milled* $SmCo_5$ + NiO with respect to ball milled $SmCo_5$ alone. These effects have been attributed to FM-AFM exchange interactions, induced by ball milling, without need of posterior field cooling processes. It is well known that, during the milling, due to the impacts between powders and balls, temperature can be locally raised to above the NiO Néel point (or strictly, to above the blocking temperature, which is always lower than T_N) [73]. Since the temperature rise is only effective during a few μs, local heating is enough to induce exchange coupling, but it is not enough to drive diffusion processes, which might lead to deterioration of $SmCo_5$ properties. Furthermore, since $SmCo_5$ particles have a large magnetocrystalline anisotropy, they can remain single-domain to very large sizes (~ 1 μm) and, therefore, they can create considerably large microscopic magnetic fields to neighboring NiO grains during the milling. Hence, field cooling can actually be thought to take place during ball milling. This effect can be considered similar to the creation of domains by local flash annealing in FM-AFM bilayers [74].

However, it is difficult to directly demonstrate the existence of FM-AFM coupling, mainly due to the magnetic and structural character of $SmCo_5$ and NiO. Namely, the magnetocrystalline anisotropy of NiO is exceedingly small to allow the existence of significant loop shifts (a clear sign of the existence of FM-AFM coupling) when coupled to $SmCo_5$. Furthermore, the $SmCo_5$ structural transitions occurring when heated, even at temperatures below T_N (NiO), impede the analysis of the temperature dependence of the coercivity enhancement (i.e. it should disappear at T_N). Moreover, the random character of the ball milled powders makes it difficult to search for unidirectional anisotropy using torque magnetometry. Therefore, the existence of FM-AFM has to be proved indirectly (see papers VI and VIII in chapter 3). Thus, for comparison, ball milling of $SmCo_5$ + CoO (CoO with similar initial grain size distribution as NiO) has been also carried out. It is noteworthy that CoO is only AFM at temperatures below room temperature, since T_N (CoO) = 290 K. Therefore, milling with CoO should not result in H_C enhancement.

The milling time dependence of H_C, measured at room temperature, for $SmCo_5$ milled alone, with NiO and with CoO (in the weight ratio of 1:1) is shown in figure 2.15. The

evolution of the magnetic properties of $SmCo_5$ when subject to ball milling has been extensively studied by several authors [67]. As can be seen in the figure, H_C is found to increase with milling time, reaching a maximum value of approximately 1.1 T after 4 h and it decreases afterwards to about 0.4 T after 32 h. The increase of H_C for short-term milling is attributed to particle size reduction, which converts them from a multidomain to a monodomain state. Nevertheless, when $SmCo_5$ is overmilled it tends to become highly disordered, losing part of its high magnetic anisotropy and thus H_C is reduced.

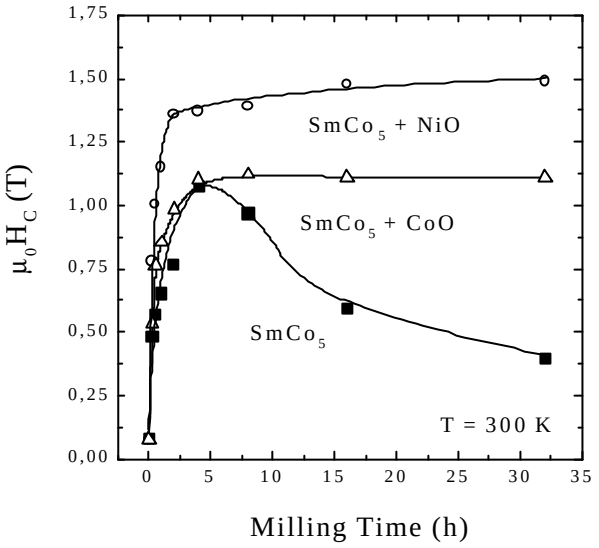

Figure 2.15: Milling time dependence of the coercivity, m_0H_C (measured at room-temperature) for ball-milled $SmCo_5$ (-■-), $SmCo_5$ + CoO 1:1 (-Δ-) and $SmCo_5$ + NiO 1:1 (-○-) powders. The lines are a guide to the eye.

Although the behavior of the three systems is similar for short milling times, it is clear that already from the early stages of milling an enhancement of H_C is observed in ball-milled $SmCo_5$ + NiO in comparison with H_C values of ball-milled $SmCo_5$ and $SmCo_5$ + CoO. Moreover, in contrast to what is observed for $SmCo_5$ alone, H_C for $SmCo_5$ + NiO and $SmCo_5$ + CoO levels off for long milling times. This is because, as has been evidenced by X- ray diffraction results, milling is less aggressive to $SmCo_5$ when it is milled together with CoO or NiO. For further discussion on this point, see papers VII and VIII in chapter 3. However, although the microstructure and morphology of $SmCo_5$ + NiO and $SmCo_5$ + CoO are rather similar, the former is found to exhibit a much larger H_C. The fact that NiO is antiferromagnetic at room-temperature (T_N = 590 K) while CoO is paramagnetic (T_N = 290 K), allows the separation of morphological-structural effects from magnetic coupling ones. Thus, the enhanced H_C should be attributed to the existence of a FM-AFM exchange coupling in the $SmCo_5$ + NiO as-milled powders.

Further proof that ball milling generates a microstructure actually suitable for FM-AFM exchange interactions, is obtained from the temperature dependence of H_C for $SmCo_5$ milled alone and together with CoO (during times exhibiting maximum H_C in each case), after field cooling ($\mu_0 H_{FC}$ = 5 T) from room temperature to 30 K (i.e. $T < T_N$ (CoO)) (see figure 2.16). As can be seen in the figure, when $SmCo_5$ + CoO (in a weight ratio of 1:1) is field cooled to low temperatures H_C increases substantially. Part of this increase is due to the changes in magnetocrystalline anisotropy of $SmCo_5$, since a similar increase in H_C is observed for $SmCo_5$ alone. Nevertheless, as expected from the FM-AFM coupling, $SmCo_5$ + CoO exhibits an extra H_C enhancement at low temperatures with respect to single $SmCo_5$ after the same field cooling procedure (i.e. at T = 30 K, after field cooling from room temperature, $\mu_0 H_C$ = 2.3 T for $SmCo_5$ + CoO, while $\mu_0 H_C$ = 1.85 T for $SmCo_5$). Moreover, the H_C enhancement in $SmCo_5$ + CoO has been found to be less if the cooling is performed in zero field (ZFC). In this case, $\mu_0 H_C$ = 2.02 T at T = 100 K, while after field cooling to the same temperature, $\mu_0 H_C$ = 2.2 T. Note that, although the local field of the $SmCo_5$ particles can induce FM-AFM coupling to the CoO even after ZFC from a demagnetized state, only those $SmCo_5$ particles which are single domain will fully contribute to it. In a field cooling experiment ($\mu_0 H_{FC}$ = 5 T) the total magnetic moment of nearly all $SmCo_5$ particles spins is aligned parallel to the applied field direction, thus all particles contribute to the coupling.

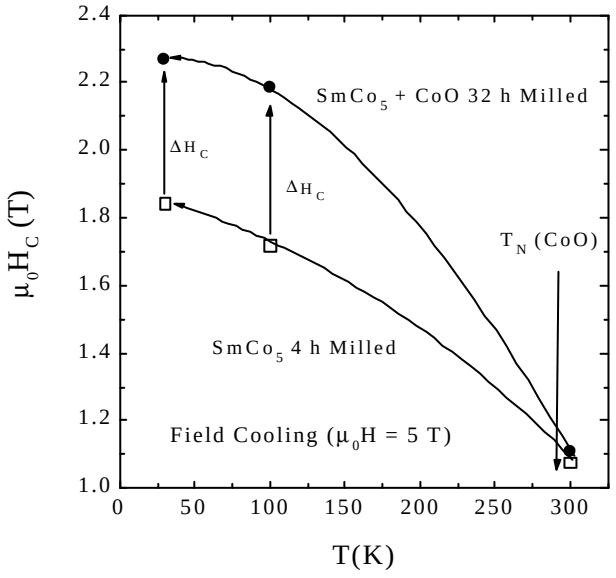

Figure 2.16: Temperature dependence of the coercivity, $\mu_0 H_C$, for $SmCo_5$ ball-milled for 4 h (-□-) and $SmCo_5$ + CoO 1:1 ball-milled for 32 h (-●-), after field cooling ($\mu_0 H_{FC}$ = 5 T) the as-milled powders to 100 K and 30 K. Also indicated is the Néel temperature of CoO (T_N = 290 K). The lines are a guide to the eye.

The difference in coercivity can also be observed in figure 2.17, where enlargements of the hysteresis loops for $SmCo_5$ milled for 4 h and $SmCo_5$ + NiO (ratio 1:1) milled for 32 h are shown.

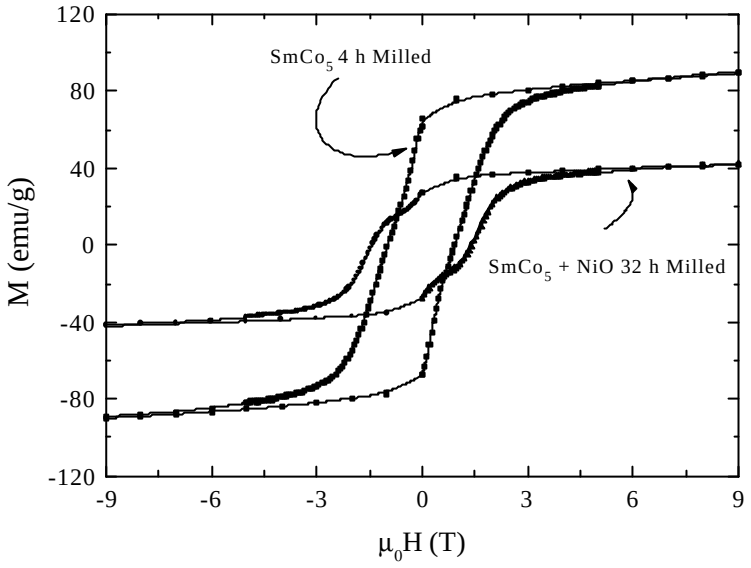

Figure 2.17: Enlargements of the hysteresis loops (in the field range from –9 to 9 T) of $SmCo_5$ and $SmCo_5$ + NiO ball milled for 4 and 32 h (in the weight ratio of 1:1), respectively.

It can be seen from figure 2.17 that, although the coercivity increases, the saturation magnetization in the case of $SmCo_5$ +NiO is reduced, due to the zero M_S of NiO (AFM). Also a shoulder is observed in $SmCo_5$ + NiO ball milled for 32 h, which is not likely to be due to the presence of two FM phases (XRD patterns show peaks corresponding to only the hard $SmCo_5$ phase), but to the existence of different regions with different degrees of coupling between the $SmCo_5$ and the NiO particles.

Furthermore, a pronounced enhancement of M_R/M_S is observed in ball milled $SmCo_5$ (either alone or with NiO or CoO), especially after short-term milling. The milling time dependences of M_R/M_S for the three systems is shown in figure 2.18. Although the Stoner-Wolfarth model for isotropic, single domain and non-interacting particles predicts a squareness of M_R/M_S = 0.5 [13], values of M_R/M_S as high as 0.9 are obtained in $SmCo_5$ milled for 0.5 h, without aligning the powders previously to magnetic measurements.

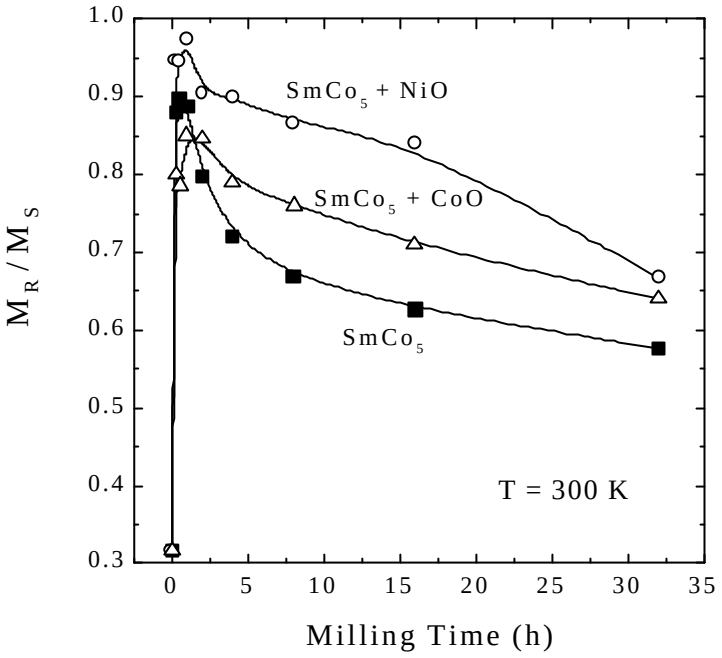

Figure 2.18: Milling time dependence of the squareness ratio, M_R/M_S (measured at room-temperature), for ball-milled $SmCo_5$ (-■-), $SmCo_5$ + CoO 1:1 (-Δ-) and $SmCo_5$ + NiO 1:1 (-○-) powders. The lines are a guide to the eye.

Remanence enhancement in isotropic FM particles has also been observed in other ball milled or melt-spun hard magnets, such as NdFeB or SmFeN [75]. This effect is usually related to short-range exchange interactions between ferromagnetic grains [76]. These exchange interactions produce a perturbed region restricted to the grain boundary where, once the field is removed, the spins remain oriented in the previous magnetizing field direction, resulting in high values of M_R. For $SmCo_5$ milled alone, M_R/M_S reaches its maximum value after 0.5 h of milling and it reduces slowly for longer milling times. This indicates that exchange interactions between FM grains have their maximum effect after short-term milling and tend to decrease afterwards. This reduction is probably due to the introduction during the milling of large amounts of defects, such as dislocations or stacking faults, which limit the extent of exchange-coupled regions within or among the FM particles. A more detailed analysis on the exchange interactions between the different FM grains or between FM and AFM grains is presented in paper IX of chapter 3.

Moreover, as shown in fig. 2.18, short-term milling of $SmCo_5$ + CoO results in somewhat lower values of M_R/M_S (compared to $SmCo_5$ milled alone or with NiO). Since CoO is paramagnetic at room-temperature, effectively its role is simply to separate the $SmCo_5$

particles, thus reducing the exchange interactions between them. The crossover at moderate milling times between the M_R/M_S of $SmCo_5$ + CoO and $SmCo_5$ alone is probably due to the more aggressive effects of the milling on $SmCo_5$ alone. Contrary to what is observed in ball-milled $SmCo_5$ + CoO, in $SmCo_5$ + NiO, M_R/M_S values even larger than the ones of $SmCo_5$ milled alone are obtained. Hence, the presence of the AFM NiO phase surrounding $SmCo_5$ seems to play an important role in further enhancing M_R/M_S. Despite that M_R/M_S enhancements have also been observed in other FM-AFM systems (e.g. Co + NiO), its origin, although clearly related to FM-AFM interactions, is not well understood. However, it seems that the interplay between FM-FM and FM-AFM exchange interactions can yield to very high M_R/M_S values.

In order to elucidate the role of NiO in the energy product enhancement, ball milling of $SmCo_5$ with NiO has been carried out varying the proportions of FM and AFM. These results are presented in paper VIII of chapter 3. The milling time dependence of H_C for $SmCo_5$ milled with NiO in the weight ratios of $SmCo_5$ (1):(0) NiO, $SmCo_5$ (3):(1) NiO, $SmCo_5$ (3):(2) NiO and $SmCo_5$ (1):(1) NiO is shown in fig. 2.19.

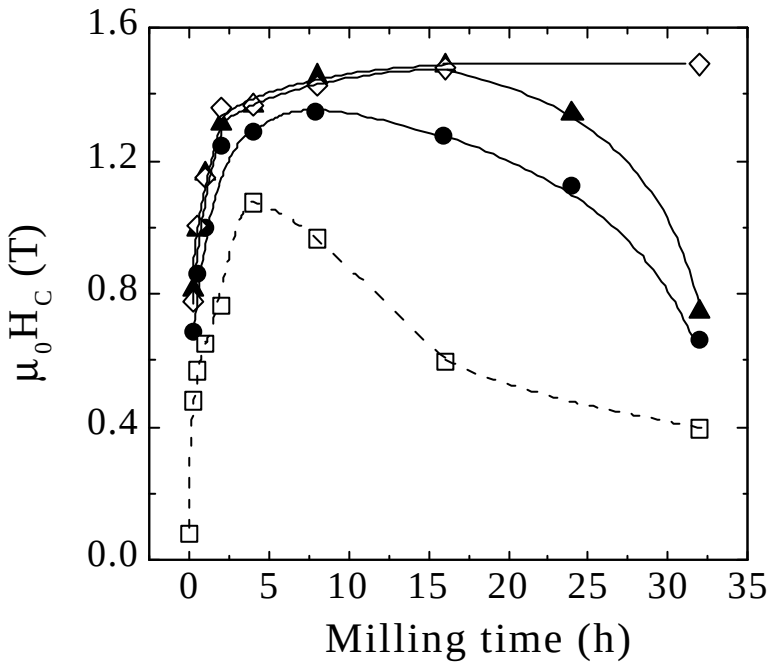

Figure 2.19: Milling time dependence of the coercivity, m_0H_C, for $SmCo_5$ milled with NiO in the weight ratios $SmCo_5$ (1):(0) NiO (-- □ --), $SmCo_5$ (3):(1) NiO (— ● —), $SmCo_5$ (3):(2) NiO (—▲ —) and $SmCo_5$ (1):(1) NiO (—◇ —). Note that the error bars are smaller than the symbols. The lines are a guide to the eye.

It can be seen that the maximum H_C is found to increase with the NiO content. This can be understood in terms of the microstructure developed in the composites. It has been observed that the $SmCo_5$ + NiO agglomerates (like the one shown in fig. 2.3), where FM-AFM exchange interactions are more likely to take place, form more easily for higher AFM contents. Moreover, the milling time at which H_C exhibits its maximum value shifts towards higher values as the NiO content is increased. This is due to the role of NiO in slowing down $SmCo_5$ structural changes, thus delaying the decrease of H_C (see fig. 2.7).

The milling time dependence of $(BH)_{Max}$ is shown in fig. 2.20 for the different FM:AFM ratios.

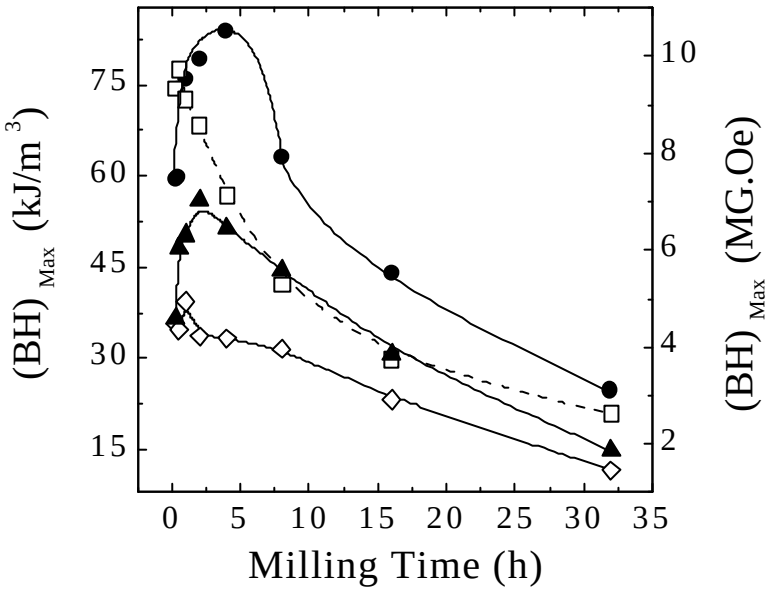

Figure 2.20: Milling time dependence of the energy product, $(BH)_{Max}$, for $SmCo_5$ milled with NiO in the weight ratios $SmCo_5$ (1):(0) NiO (-- □ --), $SmCo_5$ (3):(1) NiO (— ● —), $SmCo_5$ (3):(2) NiO (—▲—) and $SmCo_5$ (1):(1) NiO (—◇—). Given on the right axis are the $(BH)_{Max}$ values in cgs units. Note that the error bars are smaller than the symbols. The lines are a guide to the eye.

It can be observed that the dependence of $(BH)_{Max}$ on the AFM content is rather complex. This is because of the opposing effects of the AFM in the enhancement of $(BH)_{Max}$. On the one hand, both H_C and M_R/M_S increase due to the FM-AFM and FM-FM exchange interactions respectively (as for ball milled Co + NiO). On the other hand, the presence of NiO results in a reduction of the saturation magnetization of the composite, proportional to the NiO content. This stems from the zero net magnetization of the AFM (M_{AFM} = 0), which

does not contribute to the overall saturation magnetization. Consequently, as seen in fig. 2.20, $(BH)_{Max}$ is reduced when the NiO content is increasingly high, as for example in the case of the 1:1 ratio. Nevertheless, $(BH)_{Max}$ for the $SmCo_5$ (3):(1) NiO milled for 4 h exhibits an enhancement with respect to the maximum of pure $SmCo_5$. However, due to the interplay of all the different effects, an enhancement of $(BH)_{Max}$ can only be achieved through the optimization of milling time and the FM:AFM ratio.